ISSN 1870-4069

Fuzzy Segmentation and Neural Classification of Cervical Cancer Samples

Esperanza Sánchez Domínguez, Edmundo Bonilla Huerta, José Fedérico Casco Vásquez, Roberto Morales Caporal, Crispín Hernández Hernández

Tecnológico Nacional de México/Campus Apizaco, Mexico

{d04370666, edmundo.bh, depi_dci, roberto.mc, crispin.hh}
@apizaco.tecnm.mx

Abstract. In this article, a fuzzy segmentation model and a neural classification model are proposed for cervical cancer samples. The fuzzy model segments contours and nuclei of cervical cancer samples, and the neural model is aimed at classifying these samples in two stages: initial and advanced. The results obtained are very competitive for the classification of normal and abnormal cells.

Keywords: Convolutional neural networks, cervical cancer, fuzzy logic, classification.

1 Introduction

Cancer is a very common disease in our times that can start in almost any tissue or organ of the human body and begin to spread by invading other vital organs (brain, liver, kidney, lungs, cervix, etc.). The most aggressive stage in humans is metastasis, which is one of the leading causes of death. Cancer is also known as a malignant tumor or neoplasia. An alternative to make a better diagnosis is to use DNA microarray technology and thus find the main genes that cause cancer.

Cancer is the second leading cause of death worldwide and caused approximately 10 million deaths in 2020, according to the World Health Organization [1] , accounting for one in six deaths worldwide. Women are more likely to develop breast, colon, lung, cervical, and thyroid cancer. In 2022, there were around 9439 new cases of cervical cancer and 4335 deaths, making it the second most common cause of diagnosis and death for women in Mexico. There are 5.7 deaths and 12.6 morbidities per 100,000. Nonetheless, the incidence rate or morbidity has dramatically dropped from 2012 onward.

The Mexican Cancerology Institute (INCan) reported around 195,500 different types of cancer cases diagnosed each year, and 46 percent of patients die from this cause [3]. In 2022, 847,716 deaths were recorded in Mexico: 10.6% were due to malignant tumors (89,574). The death rate from this cause has increased steadily, from 62.04 deaths per 100,000 people in 2012, to 68.92 in 2022 [4].

Due to its accessibility, affordability, and ease of use, the Pap test is the most widely utilized prophylactic measure worldwide. However, its drawback is the potential for errors to emerge while interpreting the material under a microscope. An alternative for a more precise diagnosis is to use DNA microarray technology to pinpoint the most important cancer genes; however, this method is quite expensive for underdeveloped countries.

2 Related Works

In this article [5] , a systematic review of the literature from 2008 to 2020 is presented regarding the main methods for the analysis and classification of cervical cancer samples. The authors emphasize the focus of this study on works that examine the size of the cell nucleus. Normal cell nuclei are smaller than those with abnormal ones. The abnormal cell nuclei usually show disproportionate growth.

In this study [6] uses three deep learning approaches to analyze and predict cervical cancer samples. The models are validated using the technique of cross-validation and using statistical metrics. Reports indicate that the ResNet50V2 model demonstrates the highest precision.

This study [7] suggests a group of machine learning classifiers for the effective and trustworthy use of medical data in the detection of cervical cancer. The proposed approach outperforms several state-of-the-art techniques by achieving 98.06% and 95.45% accuracy for two well-known datasets, respectively. The results show that the proposed ensemble classifier can accurately identify cervical cancer and enhance diagnosis and treatment.

The novel model based on a Salp Swarm Algorithm (SSA) is proposed in [8] to improve the diagnosis of cervical cancer. This model uses well-known pre-trained models of deep learning to tackle feature extraction. Later, these predictions are integrated and optimized using SSA. The model achieves 99.48% accuracy on the Mendeley LBC dataset and 95.23% on the BloodMNIST Benchmark data set, respectively.

This research [9], addresses an approach that combines three machine learning models in a stacked ensemble voting classifier, complemented by a KNN imputation to deal with missing values. The developed model achieves performance with a precision of 0.9941, an accuracy of 0.98, a sensitivity of 0.96, and an F1 score of 0.97. For the analysis of this information, they divide model training with 70% and 30% for model testing. The system uses the XGB+RF+ETC ensemble model, which trains the XGB, RF and ETC models independently on the same data.

The article reported in [10], proposes a way to use Bradley local thresholding to find and separate nucleus cell areas in Pap smear images. The method includes color adjustment, k-means, and a modification algorithm. The nucleus cell region was segmented significantly and efficiently, with an F-measure of 98.62 percent, a sensitivity of 99.13 percent, and an accuracy of 97.96 percent.

This study [11] employs conventional machine learning (ML) concepts and a number of traditional machine learning methods, including decision trees (DT), support vector machines (SVM), logistic regression (LR), support vector machines (SVM), and K-nearest neighbors (KNN), the focus of this investigation has been cervical cancer. When it comes to cervical cancer prediction, the random forest (RF), decision tree (DT), adaptive, and gradient boosting algorithms have all produced the maximum classification score of 100% SVM, on the other hand, it has been determined to have 99% accuracy.

In this work [12], examined various supervised machine learning methods for the early detection of cervical cancer. The UCI repository's cervical cancer dataset was used to train the machine learning model. The different methods were evaluated using this dataset, which comprised 858 cervical cancer patients with 36 risk factors and one outcome variable. The XG-boost tree, random tree, logistic tree, SVM, Bayesian network, and artificial neural network were the six classification techniques used in this study. To assess the effectiveness and precision of the classifiers, all models were trained with and without a feature selection technique. Three feature selection algorithms—LASSO regression, wrapper technique, and relief rank—were employed. XG Boost, with all its features, achieved the highest accuracy of 94.94%.

3 Medical Database

To carry out the experiments, a bank of 1000 images donated by HOSPITAL GENERAL DE ZONA (HGZ 1) (IMSS, Tlaxcala) was used. The images are in JPG format, taken with optical zoom ranging from 40x to 100x with a resolution of 2592 x 1944 pixels, and are images of Pap smear tests with abnormal cells. This dataset is available on GitHub[1].

4 Methodology

The proposed model for the analysis and classification of abnormal cervical cells is shown. This model was developed using the Matlab tool version R2017a, with Toolboxes: Fuzzy Logic and Image Processing. A MacOS Sierra computer was used, with a processor: 2.9 GHz Intel Core i7 and memory: 16 GB (see figure 1).

4.1 Problem Domain

Cancer is a serious disease that affects millions of people around the world. Cancer cell sample analysis is essential for its diagnosis and treatment. This research proposes the use of fuzzy logic and artificial neural networks in the analysis of cancer cell samples. Its application in the analysis of cancer cells has the potential to improve the accuracy and efficiency of the diagnosis of images taken by Pap smear.

[1] https://github.com/EsperanzaSD/Abnormalcells

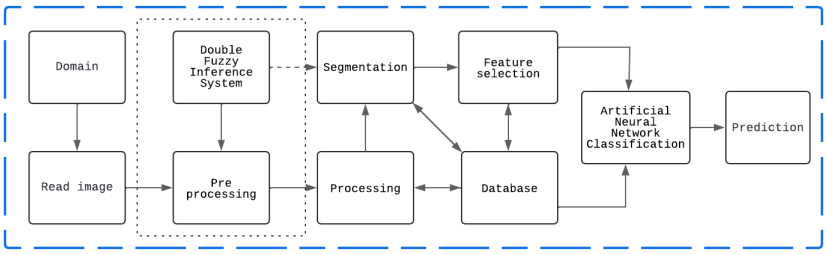

Fig. 1. Model for analysis and classification of Pap Smear samples. Source: Prepared by the authors.

Currently, the Pap test to detect cervical cancer is one of the most widely used techniques; however, these tests are sensitive to generating inaccurate information, from taking sample instruments to the interpretation of the images generated in the process. To support the diagnosis, is suggested the use of techniques with different methods that allow a statistical analysis and find characteristics in cells that are affected. The information obtained from histogram analysis can be used to extract relevant features from the image and perform in-depth interest area analysis, such as the cell nucleus and the cell.

4.2 Image Reading

Pap smear cytopathology inspection is a diagnostic technique frequently used to detect cervical cancer. A doctor collects cells from a patient's cervix with surgical brushes and then places the exfoliated cells on a glass slide during a cervical cytopathology examination. Cytopathologists use a microscope to look for malignant tumors, with each slide containing thousands of cells (Bedell et al., 2020).

For manual detection of Pap smear photos, pathologists must inspect each sub-image on a separate slide under a microscope to diagnose disease. Finding diseased cells on Pap smear cell slides can be challenging due to the similar appearance and size of some type of nuclei cells. Specialists can diagnose diseases by looking at these cells, but it depends on their experience and the cause of the disease (Sankaranarayanan et al., 2012). In Pap smear cytology, advanced interpretation techniques focus on the use of artificial intelligence to improve the accuracy of diagnoses. Using fuzzy logic and artificial neural networks makes it possible to find small patterns in tomographic images. This makes it easier to find problems earlier and detect the difference between benign and malignant lesions. Putting together systems that look at cell textures and morphology also helps with a more detailed analysis of samples, which makes for more reliable results (Alsmariy et al., 2020). Ten Pap smear images in .JPG format were used to carry out the experiments. Artificial intelligence is used for image segmentation. The image is separated into its RGB components for image processing, as it allows

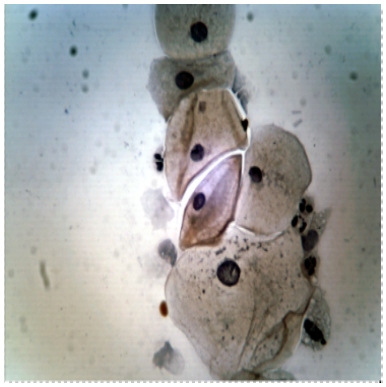

Fig. 2. Cervical cancer sample. Source: Instituto Mexicano del Seguro Social, Zona 1. Tlaxcala.

an image to be broken down into its three primary color channels (RGB): red, green, and blue. These channels are essential for the analysis and manipulation of the different characteristics of an image, such as color intensity, saturation, and brightness. Through this separation, specific patterns can be identified in each channel and individualized adjustments can be made to each of them, which is useful for information extraction. An example of a cervical cancer image is shown in the following image (see figure 2).

4.3 Pre-Processing

In this stage, a region of interest (ROI) is first defined to analyze the images of cervical cancer cells. Second, a gray level conversion is applied to facilitate the segmentation task. Third, a 3x3 convolution mask is applied to obtain the median of the image. This process smooths the gray tones of the image and reduces some noise caused during the collection stage.

4.4 Fuzzy Segmentation

Two fuzzy processing modules have been defined, the first is to detect the cell nuclei and the second is to detect the cell contour. Applying the first FIS, a fuzzy input and a fuzzy Segmented have been defined. The fuzzy input and Segmented have been partitioned into 5 fuzzy subsets, called VD: Very Dark, D: Dark, Medium, C: Clear, and VC: Very Clear. The rules are defined as follows:

1. IF Pre-processed-Image is VD THEN Segmented-Nuclei is VD,
2. IF Pre-processed-Image is D THEN Segmented-Nuclei is D,
3. IF Pre-processed-Image is M THEN Segmented-Nuclei is M,
4. IF Pre-processed-Image is C THEN Segmented-Nuclei is D,
5. IF Pre-processed-Image is VC THEN Segmented-Nuclei is M.

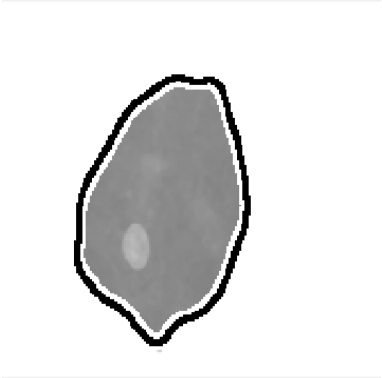

Fig. 3. Feature selection stage of segmented contour of normal cell of Pap smear sample.

The purpose of these rules is to emphasize darker shades in order to facilitate cell nuclei segmentation. The following rules defined for the second fuzzy processing aim to enhance contrast in dark regions and soften light regions:

1. IF Pre-processed-Image is VD THEN Segmented-Contour is VD,
2. IF Pre-processed-Image is D THEN Segmented-Contour is VD,
3. IF Pre-processed-Image is M THEN Segmented-Contour is D,
4. IF Pre-processed-Image is C THEN Segmented-Contour is M,
5. IF Pre-processed-Image is VC THEN Segmented-Contour is C.

Using this second fuzzy inference module, the contrast of dark regions is significantly improved, and light regions are smoothed, thus facilitating cell contour segmentation.

4.5 Feature Selection

The results of double fuzzy processing are what make up the feature selection process. This means that we have the segmented cell as well as the cell nucleus of all cervical cancer samples in the image database. Figure 3 illustrates the feature selection of an early-stage cancer sample.

4.6 Convolutional Neural Network

In this work, we propose a Convolutional Neural Network (CNN) to classify 200 samples of cancer contours of the Pap smear cervix. 100 samples are normal and 100 samples are abnormal, respectively. The proposed architecture consists of several convolutional layers (see Figure 4). The images from input data (1944x2592x3) of layer 0 were pre-processed and rescaled to 130x130x3, it is recommended that images must be square, to reduce the cost in CNN architecture. The follow step is to feed the first layer of convolution that consist of 32 filters of 3x3 and to move this filters to scan the image, for this task we

define a stride of size 1. The result of this convolutional process is a matrix of 130x130x64. To reduce this data preserving the most relevant features of data is to use a pooling layer stacked after the convolutional layer.

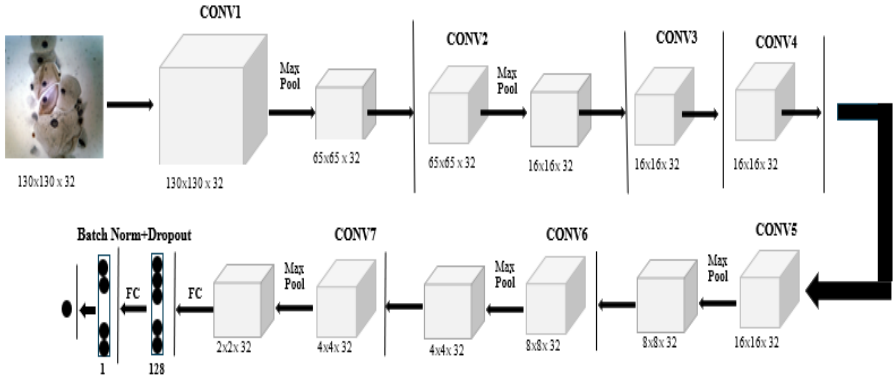

Fig. 4. The architecture of CNN.

```
Model: "sequential"
_________________________________________________________________
Layer (type)                 Output Shape              Param #
=================================================================
conv2d (Conv2D)              (None, 130, 130, 32)      896
_________________________________________________________________
max_pooling2d (MaxPooling2D) (None, 65, 65, 32)        0
_________________________________________________________________
conv2d_1 (Conv2D)            (None, 65, 65, 32)        9248
_________________________________________________________________
max_pooling2d_1 (MaxPooling2 (None, 32, 32, 32)        0
_________________________________________________________________
conv2d_2 (Conv2D)            (None, 32, 32, 32)        9248
_________________________________________________________________
max_pooling2d_2 (MaxPooling2 (None, 16, 16, 32)        0
_________________________________________________________________
conv2d_3 (Conv2D)            (None, 16, 16, 32)        9248
_________________________________________________________________
conv2d_4 (Conv2D)            (None, 16, 16, 32)        9248
_________________________________________________________________
conv2d_5 (Conv2D)            (None, 16, 16, 32)        9248
_________________________________________________________________
max_pooling2d_3 (MaxPooling2 (None, 8, 8, 32)          0
_________________________________________________________________
conv2d_6 (Conv2D)            (None, 8, 8, 32)          9248
_________________________________________________________________
max_pooling2d_4 (MaxPooling2 (None, 4, 4, 32)          0
_________________________________________________________________
conv2d_7 (Conv2D)            (None, 4, 4, 32)          9248
_________________________________________________________________
max_pooling2d_5 (MaxPooling2 (None, 2, 2, 32)          0
_________________________________________________________________
flatten (Flatten)            (None, 128)               0
_________________________________________________________________
dense (Dense)                (None, 128)               16512
_________________________________________________________________
activation (Activation)      (None, 128)               0
_________________________________________________________________
dropout (Dropout)            (None, 128)               0
_________________________________________________________________
dense_1 (Dense)              (None, 1)                 129
_________________________________________________________________
activation_1 (Activation)    (None, 1)                 0
=================================================================
Total params: 82,273
Trainable params: 82,273
Non-trainable params: 0
```

Fig. 5. Summary of CNN proposed.

```
Epoch 95/100
1/1 [==============================] - 5s 5s/step - loss: 0.0191 - accuracy: 1.0000 - val_loss: 1.0602 - val_accuracy: 0.7000
Epoch 96/100
1/1 [==============================] - 5s 5s/step - loss: 0.0898 - accuracy: 0.9500 - val_loss: 0.9719 - val_accuracy: 0.8500
Epoch 97/100
1/1 [==============================] - 5s 5s/step - loss: 0.0748 - accuracy: 1.0000 - val_loss: 0.5246 - val_accuracy: 0.8500
Epoch 98/100
1/1 [==============================] - 7s 7s/step - loss: 0.0733 - accuracy: 1.0000 - val_loss: 1.1425 - val_accuracy: 0.7500
Epoch 99/100
1/1 [==============================] - 5s 5s/step - loss: 0.0437 - accuracy: 1.0000 - val_loss: 0.7489 - val_accuracy: 0.8500
Epoch 100/100
1/1 [==============================] - 5s 5s/step - loss: 0.0268 - accuracy: 1.0000 - val_loss: 0.7177 - val_accuracy: 0.8500
```

Fig. 6. Results of training and testing.

The max-pooling layer is defined a 2x2 filter and a stride of 2, the result of this process is a 64x64x64 size feature matrix. We use many Max-pooling layers in our architecture to reduce significantly the CNN time execution to obtain better results.

We also include a dropout layer in the architecture to improve the generalization capacities of our model. In this step, the dropout factor is fixed to 0.5. Thus, we have the basic CNN model, which includes seven convolutional layers, a max-pooling layer and a dropout layer to create a convolutional cycle.

After seven convolutions the resultant matrix of Pap smear images matrix becomes a $2 \times 2 \times 32$. This resultant matrix is flattened to obtain a feature vector of size 128. The last layer contains only 2 neurons with a sigmoid function. Different cycles are proposed in the architecture to reduce the feature size of Pap smear samples and thus to facilitate binary classification (initial and advanced). CNN proposed summary is shown in figure 5.

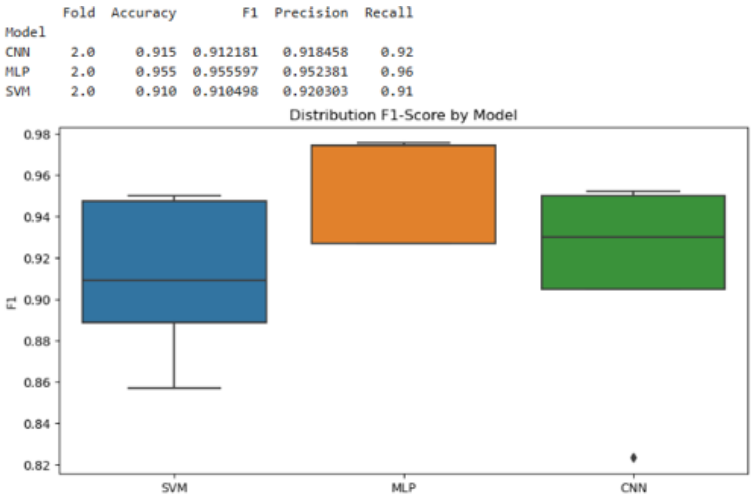

Fig. 7. Results of samples.

5 Results

Our model achieves 100% accuracy in the training data before reaching the defined number of epochs, gradually decreasing accuracy at epoch 97, and stabilizing again at the 98 training epoch. We define a limit of 100 epoch for this model (See Figure 6).

In this experimentation protocol, we use the binary cross entropy loss and the Adam optimizer to validate CNN.

6 Comparaison with Other Works

To validate our model with other works reported in the literature, we selected the well-known SIPAKMED biomedical database, which contains 4,049 cell images from five types of cervical cancer. The authors [13] simplified the classification process for these five classes into two (normal and abnormal). We applied our model, and the results are shown in figure 7.

Table 1. Comparison with other similar works using only two classes.

Method	accuracy	precision	recall	F_1 score
AlexNet, GAN [14]				
93.8%	47.8%	95.9%	93.6%	94.1%
CNN-PCA [15]				
–	–	–	ResNet-152 [2] 94.8%	–
–	–	MLP-Nuclei [13] 78.8%	–	–
–	MLP-Cytoplasm [13] 83.4%	–	–	– SVM-Nuclei [13]
88.5%	–	–	–	91.6%
SVM-Cytoplasm [13]				
–	–	–	CNN-RGB [13] 95.3%	–
–	–	our model and CNN 91.5%	91.8%	92.0%
91.8% our model and MLP	**95.5%**	**95.2%**	**96.0%**	**95.5%** our model and SVN
91.0%	92.0%	91.0%	91.0%	

Using our model that combines two fuzzy segmentations (nuclei and contour) and three different classifiers (CNN, MLP, and SVM), we find that the MLP

classifier gives the best results, achieving a precision of 95%, an F1 score of 95.5%, a precision of 95.23%, and a recall of 96.0% (see figure 7).

In Table 1, we summarize our model's results alongside other similar studies that used the SIPAKMED dataset. In Table 1 are summarized results of our model with other similar works reported in the literature using the SIPAKMED dataset. We evaluated the performance of the proposed model using the 5-fold cross-validation method. We observed that our model for binary classification outperforms other comparable works using the same dataset.

7 Conclusions

We present in this paper a double fuzzy inference system that can help to find two features about Pap smear samples for cervix cancer: contour nuclei and contour cells. To obtain better results using a convolutional neural network (CNN), we use in this work the contour of normal and abnormal samples and thus reduce the computation time. In future work, we intend to perform a multi-classification of cervical cancer samples for monitoring at each stage.

References

1. World Health Organization: Cancer. (2019, July 12). Retrieved from https://onx.la/4e793
2. Tripathi, A., Arora, A., Bhan, A.: Classification of cervical cancer using Deep Learning Algorithm. In: 5th International Conference On Intelligent Computing And Control Systems (ICICCS), pp. 1210–1218 (2021)
3. Instituto Nacional de Cancerología (INCan): 294: México registra al año más de 195 mil casos de cáncer: Secretaría de Salud. (2023) Retrieved from: https://onx.la/df378
4. Instituto Nacional de Estadística y Geografía Estadística a propósito del día mundial contra el cáncer. (2024) Retrieved from https://onx.la/b6708
5. Wei, L., Mustafa, W., Jamlos, M., Idrus, S., Sahabudin, M.: Cervical cancer classification using image processing approach: A review. In: IOP Conference Series: Materials Science And Engineering, 917, 012068 (2020) https://doi.org/10.1088/1757-899X/917/1/012068.
6. Devaraj, S., Madian, N., Menagadevi, M., Remya, R.: Deep learning approaches for analysing papsmear images to detect cervical cancer. In: Wireless Personal Communications, 135, 81–98 (2024) https://doi.org/10.1007/s11277-024-10986-8.
7. Ali, M., Hossain, M., Kona, M., Nowrin, K., Islam, M.: An ensemble classification approach for cervical cancer prediction using behavioral risk factors. Healthcare Analytics, 5 pp. 100324 (2024). https://doi.org/10.1016/j.health.2024.100324.
8. Bilal, O., Asif, S., Zhao, M., Khan, S., Li, Y.: An amalgamation of deep neural networks optimized with Salp swarm algorithm for cervical cancer detection. Computers And Electrical Engineering, 123, pp. 110106 (2025) https://doi.org/10.1016/j.compeleceng.2025.110106.
9. Aljrees, T.: Improving prediction of cervical cancer using KNN imputer and multi-model ensemble learning. Plos One, 19, e0295632 (2024) https://doi.org/10.1371/journal.pone.0295632.

10. Halim, A., Mustafa, W., Nasir, A., Ismail, S., Alquran, H.: Nucleus Cell Segmentation on Pap Smear Image using Bradley Modification Algorithm. Neural Network World, (2024) https://doi.org/10.14311/NNW.2024.34.003.
11. Al Mudawi, N., Alazeb, A.: A model for predicting cervical cancer using machine learning algorithms. Sensors, 22, 4132 (2022) https://doi.org/10.3390/s22114132.
12. Kumawat, G., Vishwakarma, S., Chakrabarti, P., Chittora, P., Chakrabarti, T., Lin, J.: Prognosis of cervical cancer disease by applying machine learning techniques. Journal of Circuits, Systems and Computers, 32, 2350019 (2023) https://doi.org/10.1142/S0218126623500196.
13. Plissiti, M., Dimitrakopoulos, P., Sfikas, G., Nikou, C., Krikoni, O., Charchanti, A.: Sipakmed: A new dataset for feature and image based classification of normal and pathological cervical cells in pap smear images. In: 2018 25th IEEE International Conference On Image Processing (ICIP), pp. 3144–3148 (2018)
14. Yu, S., Zhang, S., Wang, B., Dun, H., Xu, L., Huang, X., Shi, E., Feng, X.: Generative adversarial network based data augmentation to improve cervical cell classification model. Math. Biosci. Eng., 18, 1740–1752 (2021)
15. Al-asbaily, S., Almoshity, S., Younus, S., Bozed, K.: Classification of Cervical Cancer using Convolutional Neural Networks. In: 2024 IEEE 4th International Maghreb Meeting Of The Conference On Sciences And Techniques Of Automatic Control And Computer Engineering (MI-STA), pp. 735–739 (2024)